

Learning by Watching: Physical Imitation of Manipulation Skills from Human Videos

Haoyu Xiong^{*†}, Quanzhou Li^{*}, Yun-Chun Chen^{*}, Homanga Bharadhwaj^{*}, Samarth Sinha^{*}, Animesh Garg^{*‡}

Abstract—We present an approach for physical imitation from human videos for robot manipulation tasks. The key idea of our method lies in explicitly exploiting the kinematics and motion information embedded in the video to learn structured representations that endow the robot with the ability to imagine how to perform manipulation tasks in its own context. To achieve this, we design a perception module that learns to translate human videos to the robot domain followed by unsupervised keypoint detection. The resulting keypoint-based representations provide semantically meaningful information that can be directly used for reward computing and policy learning. We evaluate the effectiveness of our approach on five robot manipulation tasks, including reaching, pushing, sliding, coffee making, and drawer closing. Detailed experimental evaluations demonstrate that our method performs favorably against previous approaches. More results and analysis are available at pair.toronto.edu/lbw-kp/.

I. INTRODUCTION

Robotic *Imitation Learning*, also known as *Learning from Demonstration* (LfD), allows robots to acquire manipulation skills guided by expert demonstrations through learning algorithms. Despite the recent progress, collecting expert demonstrations remains expensive and challenging as it assumes access to both observations and actions via kinesthetic teaching [1], [2], teleoperation [3], [4], or crowdsourcing platform [5]–[8]. In contrast, humans have the ability to imitate manipulation skills by *watching* third-person performances. Motivated by this, we aim to endow robots with the ability to learn manipulation skills via physical imitation from human videos.

Unlike typical LfD methods [1]–[4], which assume access to both expert observations and actions, we relax this supervision to human videos alone. One of the main challenges is the domain gap between a human video and the robot environment. For instance, human arms typically do not match the morphology of the robot arms. One way to bridge the human-robot domain gap is to translate the human videos to the robot domain using a generative modeling approach [9]–[11]. Simple generative models do not capture all the semantics from images and tend to omit hard-to-model features that may be important for the task [12].

The goal of this work is to investigate how to learn semantic representations that allow the robot to 1) represent the task in its own context, and 2) omit artifacts caused by the human-robot translation in an unsupervised fashion. In order to achieve this, we propose *Learning by Watching* (LbW). The key component of our framework is the perception module

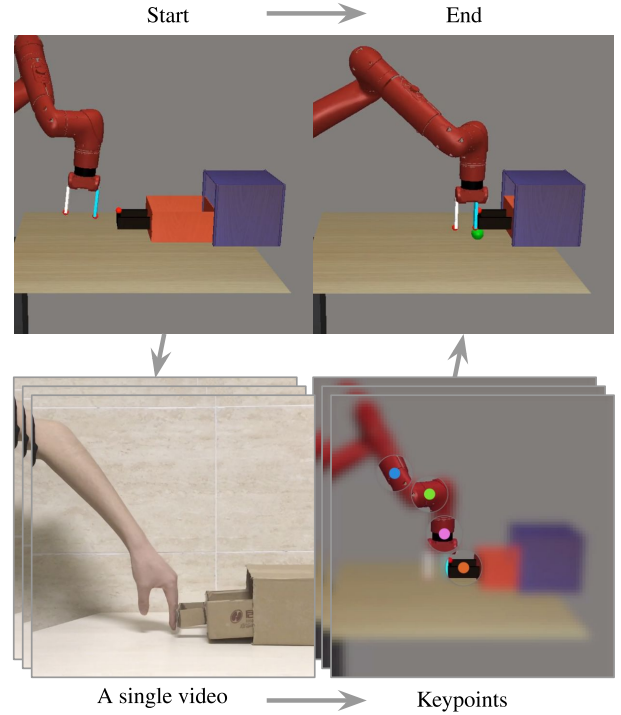


Fig. 1: **LbW**. To achieve physical imitation from human videos, our key intuition is to learn a structured representation captured by keypoints that provides semantically meaningful information for robot manipulation tasks. The resulting representations is then used to compute reward and perform policy learning, carrying out the learning of physical imitation from human videos.

that explicitly learns semantic representations via unsupervised keypoint detection. As shown in Figure 1, the perception module enables the robot to imagine how to perform a task by establishing correspondences between human and robot via translation followed by keypoint detection. The detected keypoints can represent the robot arm pose and the interacting object while ignoring task-irrelevant distractors. Besides, the learned keypoint-based representations are directly used for inferring the task reward from a single human video with a simple distance metric. By this learned reward model, we achieve imitation from human videos via reinforcement learning.

Detailed experimental evaluations on five robot manipulation tasks, including reaching, pushing, sliding, coffee making, and drawer closing, show that our method performs favorably against previous works.

Our contributions can be summarized as follows:

- 1) We propose a perception module for physical imitation from human videos using human to robot translation

^{*}University of Toronto & Vector Institute, [†]Tianjin University, [‡]Nvidia.

and unsupervised keypoint detection.

- 2) The resulting keypoint-based representations can be used to compute the task reward with a simple distance metric.
- 3) Experimental results on five robot manipulation tasks show that our method greatly outperforms previous works.

II. RELATED WORK

Imitation from human videos. Most prior imitation learning approaches [13] collect demonstrations by using kinesthetic teaching [1], [2], teleoperation [3], [4], or by crowdsourcing platform [5]–[8], and crucially assume access to both observations and actions at every time step.

Recent progress in deep representation learning has accelerated developments in imitation from videos [9]–[11], [14]–[21]. Achieving imitation from human videos via translation methods is not a new idea. However, human-robot paired training data is needed in most of the approaches [9], [11].

Closely related to our work, Laura et al. propose a method [10] to convert human demonstrations to robot domain with unpaired training data via CycleGAN [22]. In contrast to this work, the keypoints-based representations in our method can endure the artifacts created by imperfect translation, thereby leading to better performance for downstream control.

Different from translation methods, Maximilian et al. [20] leverage 3D detection to bridge the visual gap between human and robot. SFV [19] enables humanoid characters to learn skills from videos based on deep pose estimation. These works share a similar reward computing metric like ours. While in these works, pre-trained detection models need label data, our model learns in an unsupervised manner.

Image-to-image translation. Generative adversarial networks [23] have been successfully applied to image-to-image translation. CycleGAN [22] learns to translate images in an unpaired data setting by exploiting the idea of cycle consistency. UNIT [24] achieves image-to-image translation by assuming a shared latent space between the two domains. Other methods explore translating images across multiple domains [25] or learning to generate diverse outputs [26]–[28]. Recently, image-to-image translation approaches are applied to address various problems such as domain adaptation [29]–[31] and policy learning [10], [32]. In our work, we leverage MUNIT [28] to perform human to robot translation for achieving physical imitation from human videos.

Unsupervised keypoint detection. Detecting keypoints from images without supervision has been studied in the literature [33], [34]. In the context of computer vision, existing methods typically infer keypoints by assuming access to the temporal transformation between video frames [33] or employing a differentiable keypoint bottleneck network without access to frame transitions information [34]. Other approaches estimate keypoints based on the access to known image transformations and dense correspondences between features [35]–[37].

Apart from the aforementioned approaches, some recent methods focus on learning keypoint detection for image-based control tasks. Examples include detecting keypoints based

on single frame reconstruction with fully connected neural networks without learning object-centric latent representations [38] and leveraging object motions to transport features at the detected keypoint locations [39]. In our method, we adopt Transporter [39] to detect keypoints in an unsupervised manner.

III. PRELIMINARIES

To achieve physical imitation from human videos, we decompose the problem into a series of tasks: 1) human to robot translation, 2) unsupervised keypoint-based representation learning, and 3) physical imitation with RL. Here, we review the first two tasks, in which our method builds upon existing algorithms.

A. Unsupervised Image-to-Image Translation

Similar to existing methods [9], [10], we cast robot to human translation as an unsupervised image-to-image translation problem. Specifically, we aim to learn a model that translates images from a source domain X (e.g., human domain) to a target domain Y (e.g., robot domain) without paired training data [22], [24], [27], [28]. In our method, we adopt MUNIT [28] as the image-to-image translation network to achieve human to robot translation. MUNIT learns to translate images between the two domains by assuming that an image representation can be disentangled into a domain-invariant content code (encoded by a content encoder E^c) and a domain-specific style code (encoded by a style encoder E^s). The content encoders E_X^c and E_Y^c are shared in the two domains, whereas the style encoders E_X^s and E_Y^s of the two domains do not share weights. To translate an image from one domain to the other, we combine its content code with a style code sampled from the other domain. The translations are learned to generate images that are indistinguishable from images in the translated domain. Given an image x from the source domain X and an image y from the target domain Y , we define the adversarial loss $\mathcal{L}_{\text{GAN}}^x$ in the source domain as

$$\mathcal{L}_{\text{GAN}}^x = \mathbb{E} \left[\log D_X(x) + \log \left(1 - D_X(G_X(c_y, s_x)) \right) \right], \quad (1)$$

where $c_y = E_Y^c(y)$ is the content code of image y , $s_x = E_X^s(x)$ is the style code of image x , G_X is a generator that takes as input a content code c_y and a style code s_x and generates images that have similar distributions like those in the source domain, and D_X is a discriminator that aims to distinguish between the translated images generated by G_X and the images in the source domain. The adversarial loss $\mathcal{L}_{\text{GAN}}^y$ in the target domain can be similarly defined.

In addition to the adversarial losses, MUNIT applies reconstruction losses on images and content and style codes to regularize the model learning. For the source domain, the image reconstruction loss $\mathcal{L}_{\text{rec}}^x$ is defined as

$$\mathcal{L}_{\text{rec}}^x = \mathbb{E} \left[\|G_X(c_x, s_x) - x\| \right], \quad (2)$$

the content reconstruction loss $\mathcal{L}_{\text{rec}}^{c_x}$ is defined as

$$\mathcal{L}_{\text{rec}}^{c_x} = \mathbb{E} \left[\|E_Y^c(G_Y(c_x, s_y)) - c_x\| \right], \quad (3)$$

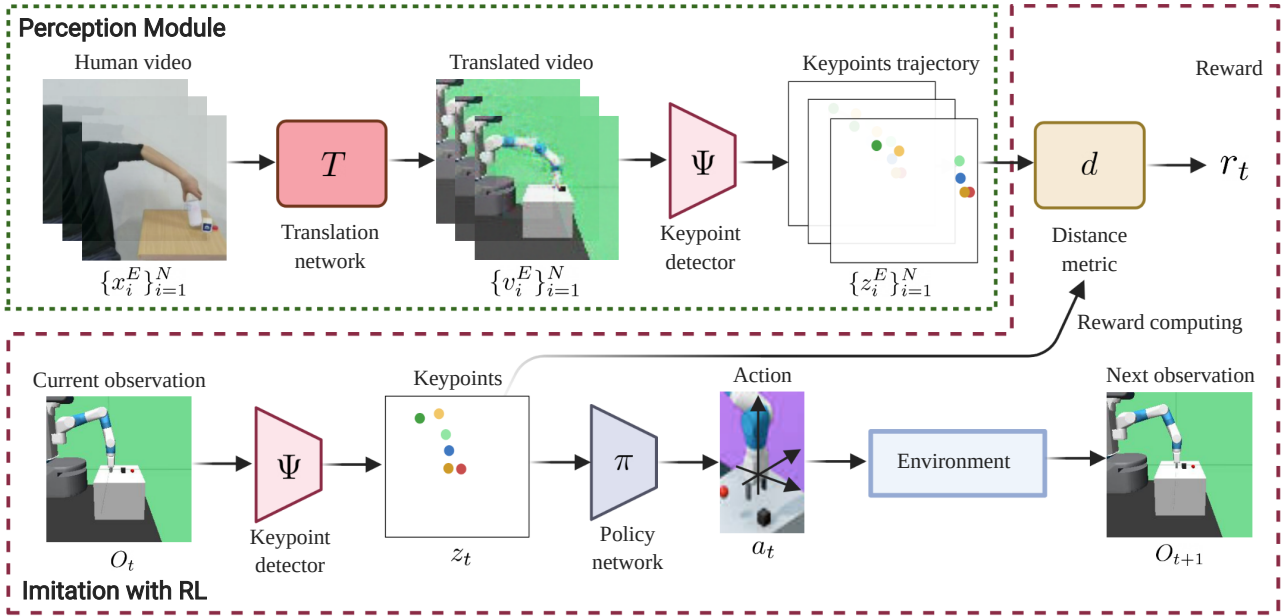


Fig. 2: **Overview of the proposed LbW.** Our LbW model is composed of three main components: an image-to-image translation network T , a keypoint detector Ψ , and a policy network π . The image-to-image translation network translates the input human demonstration video frame by frame to generate a robot demonstration video. Next, the keypoint detector takes the generated robot demonstration video as input and extracts the keypoint-based representation for each frame to form a keypoints trajectory. At each time step, the keypoint detector also extracts the keypoint-based representation for the current observation. The reward for physical imitation is defined by a distance metric d that measures the distance between the keypoint-based representation of the current observation and those in the keypoints trajectory. Finally, the keypoint-based representation of the current observation are passed to the policy network to predict an action that is used to interact with the environment.

and the style reconstruction loss $\mathcal{L}_{\text{rec}}^{s_x}$ is defined as

$$\mathcal{L}_{\text{rec}}^{s_x} = \mathbb{E} \left[\left\| E_X^s(G_X(c_y, s_x)) - s_x \right\| \right]. \quad (4)$$

The image reconstruction loss $\mathcal{L}_{\text{rec}}^y$, the content reconstruction loss $\mathcal{L}_{\text{rec}}^{c_y}$, and the style reconstruction loss $\mathcal{L}_{\text{rec}}^{s_y}$ in the target domain can be derived similarly.

The total loss $\mathcal{L}_{\text{MUNIT}}$ for training MUNIT is given by

$$\mathcal{L}_{\text{MUNIT}} = \mathcal{L}_{\text{GAN}}^x + \mathcal{L}_{\text{GAN}}^y + \lambda_{\text{image}}(\mathcal{L}_{\text{rec}}^x + \mathcal{L}_{\text{rec}}^y) + \lambda_{\text{content}}(\mathcal{L}_{\text{rec}}^{c_x} + \mathcal{L}_{\text{rec}}^{c_y}) + \lambda_{\text{style}}(\mathcal{L}_{\text{rec}}^{s_x} + \mathcal{L}_{\text{rec}}^{s_y}), \quad (5)$$

where λ_{image} , λ_{content} , and λ_{style} are hyperparameters used to control the relative importance of the respective loss functions.

B. Unsupervised Keypoint Detection

To perform control tasks, existing approaches typically resort to learning state representations based on image observations [10], [40]–[43]. While promising results have been presented, the state representation learning in these methods does not consider kinematics of the robot arm (i.e., robot arm pose) and the motion of the interacting object which are useful for control tasks, leading to sub-optimal performance. In contrast to these approaches, we *explicitly* exploit the kinematics and motion information embedded in robot videos and adopt Transporter [39] to detect the keypoints in each video frame in an unsupervised fashion. The detected keypoints form a structured representation that captures the robot arm pose and the location of the interacting object, providing semantically meaningful information for control tasks.

To realize the learning of unsupervised keypoint detection, Transporter leverages object motion between a pair of video frames to transform a video frame into the other by transporting features at the detected keypoint locations. Given two video frames x and y , Transporter first extracts feature maps $\Phi(x)$ and $\Phi(y)$ for both video frames using a feature encoder Φ and detects K 2-dimensional keypoint locations $\Psi(x)$ and $\Psi(y)$ for both video frames using a keypoint detector Ψ . Transporter then synthesizes the feature map $\hat{\Phi}(x, y)$ by suppressing the feature map of x around each keypoint location in $\Psi(x)$ and incorporating the feature map of y around each keypoint location in $\Psi(y)$:

$$\hat{\Phi}(x, y) = (1 - \mathcal{H}_{\Psi(x)}) \cdot (1 - \mathcal{H}_{\Psi(y)}) \cdot \Phi(x) + \mathcal{H}_{\Psi(y)} \cdot \Phi(y), \quad (6)$$

where $\mathcal{H}_{\Psi(\cdot)}$ is a Gaussian heat map with peaks centered at each keypoint location in $\Psi(\cdot)$.

Next, the transported feature $\hat{\Phi}(x, y)$ is passed to a refinement network R to reconstruct to the video frame y . We define the loss $\mathcal{L}_{\text{transporter}}$ for training Transporter as

$$\mathcal{L}_{\text{transporter}} = \mathbb{E} \left[\left\| R(\hat{\Phi}(x, y)) - y \right\| \right]. \quad (7)$$

In the next section, we leverage the Transporter model to detect keypoints for each video frame. The detected keypoints are then used as a structured representation for defining the reward function and as the input of the policy network to predict an action that is used to interact with the environment.

IV. PROPOSED METHOD

In this section, we first provide an overview of our approach. We then describe the unsupervised domain transfer with

keypoint-based representations module. Finally, we describe the details of physical imitation with RL.

A. Algorithmic Overview

We consider the task of physical imitation from human videos for robotic manipulation tasks. In this setting, we assume we have access to a *single* human demonstration video $V_X = \{x_i^E\}_{i=1}^N$ of length N depicting a human performing a specific task (e.g., pushing a block) that we want the robot to learn from, where $x_i^E \in \mathbb{R}^{H \times W \times 3}$ and $H \times W$ is the spatial size of x_i^E . We note that the human actions are *not* given in our setting. Our goal is to develop a learning algorithm that allows the robot to *imitate* the behavior demonstrated by the human in the human demonstration video V_X . To achieve this, we present LbW which comprises three components: 1) the image-to-image translation network T (from MUNIT [28]), 2) the keypoint detector Ψ (from the keypoint detector of Transporter [39]), and 3) the policy network π . As shown in Figure 2, given a human demonstration video V_X and the current observation $O_t \in \mathbb{R}^{H \times W \times 3}$ at time t , we first apply the image-to-image translation network T to each frame x_i^E in the human demonstration video V_X and translate x_i^E to a robot demonstration video frame $v_i^E \in \mathbb{R}^{H \times W \times 3}$. Next, the keypoint detector Ψ takes each translated robot video frame v_i^E as input and extracts the keypoint-based representation $z_i^E = \Psi(v_i^E) \in \mathbb{R}^{K \times 2}$, where K denotes the number of keypoints. Similarly, we also apply the keypoint detector Ψ to the current observation O_t to extract the keypoint-based representation $z_t = \Psi(O_t) \in \mathbb{R}^{K \times 2}$. To compute the reward for physical imitation, we define a distance metric d that computes the distances between the keypoint-based representation z_t of the current observation O_t and each of the keypoint-based representations z_i^E of the translated robot video frames v_i^E . Finally, the policy network π takes as input the keypoint-based representation z_t of the current observation O_t to predict an action $a_t = \pi(z_t)$ that is used to guide the robot to interact with the environment. The details of each component are described in the following subsections.

B. Unsupervised Domain Transfer with Keypoints

To achieve physical imitation from human videos, we develop a perception module that consists of a MUNIT model for human to robot translation and a Transporter network for keypoint detection as shown in Figure 3. To train the MUNIT model, we first collect the training data for the source domain (i.e., human domain) and the target domain (i.e., robot domain). The source domain contains the human demonstration video V_X that we want the robot to learn from. To increase the diversity of the training data in the source domain for facilitating the MUNIT model training, we follow AVID [10] and collect a few *random* data by asking the human to randomly move the hands above the table *without* performing the task. As for the target domain training data, we collect a number of robot videos generated by having the robot perform a number of actions that are randomly sampled from the action space. As such, the collection of the robot videos does *not* require human expertise and effort. Using the training

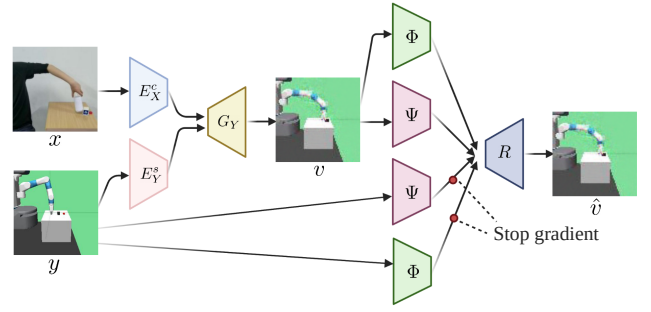


Fig. 3: **Overview of the perception module.** Our perception module is composed of a MUNIT network (left) and a Transporter model (right). Given a human video frame x and a robot video frame y , the MUNIT model first extracts the content code of the human video frame and the style code of the robot video frame. The MUNIT model then generates the translated robot video frame v by combining the extracted content code and style code. Next, the Transporter model extracts the features and detects the keypoints for both the translated robot video frame v and the input robot video frame y and reconstructs the translated robot video frame \hat{v} by transporting features at the detected keypoint locations. Note that the input robot video frame y are from a robot video generated by using a random policy.

data from both source and target domains, we are able to train the MUNIT model to achieve human to robot translation using the total loss $\mathcal{L}_{\text{MUNIT}}$ in (5) and following the protocol described in Section III-A. After training the MUNIT model, we are able to translate the human demonstration video $V_X = \{x_i^E\}_{i=1}^N$ frame by frame to the robot demonstration video $\{v_i^E\}_{i=1}^N$ by combining the content code of each human demonstration video frame and a style code randomly sampled from the robot domain.

As mentioned in Section III-B, we aim to leverage the kinematics information of the robot arm and the motion information of the interacting object when performing physical imitation for robot manipulation tasks. To achieve this, we leverage Transporter to learn a keypoint-based representation in an unsupervised fashion, as there are no ground-truth keypoint annotations available. As illustrated in Figure 3, following the protocol stated in Section III-B, the Transporter model takes as input a translated robot demonstration video frame v and a robot video frame y from a robot video collected by applying a random policy and extracts their features and detects keypoint locations, respectively. The Transporter model then reconstructs the translated robot demonstration video frame. To train the Transporter model, we optimize the total loss $\mathcal{L}_{\text{transporter}}$ in (7). Once the training of the Transporter model converges, we are able to use the keypoint detector Ψ of the Transporter model to extract a keypoint-based representation $z_i^E = \Psi(v_i^E)$ for each frame v_i^E in the translated robot demonstration video to form a keypoints trajectory $\{z_i^E\}_{i=1}^N$ and a keypoint-based representation $z_t = \Psi(O_t)$ for the current observation O_t . The keypoints trajectory $\{z_i^E\}_{i=1}^N$ of the translated robot demonstration video $\{v_i^E\}_{i=1}^N$ and the keypoint-based representation z_t of the current observation O_t provide *semantically* meaningful information for robot manipulation tasks. We then use both of them to compute the reward r_t

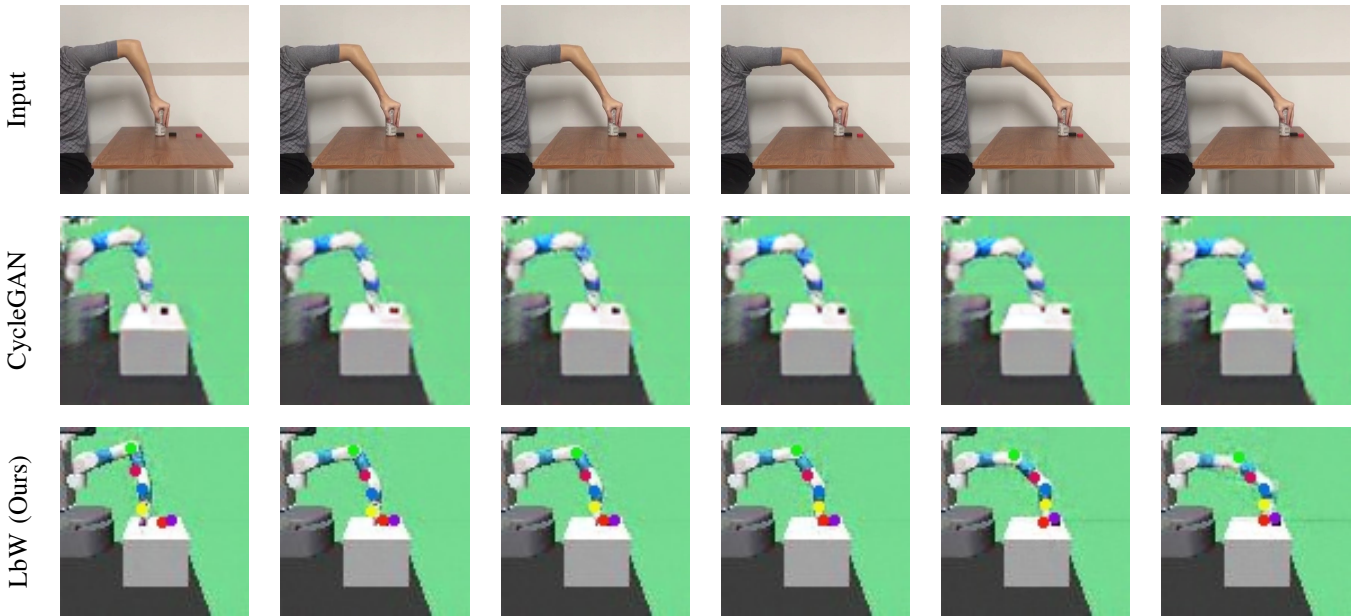


Fig. 4: **Visual results and comparisons on the pushing task.** Given a human video as input in the first row, we present the translated images of CycleGAN [22] in the second row. In the third row, we visualize our translated images and the detected keypoints produced by the perception module. Our perception module accurately detects the robot arm pose and the location of the interacting object.

and use the keypoint-based representation z_t of the current observation O_t predict an action a_t used to interact with the environment. The details of reward computing and policy learning are elaborated in the next subsection.

C. Physical Imitation with RL

To control the robot, we use RL to learn a policy from image-based observations that maximize the cumulative values of a learned reward function. In our method, we *decouple* the policy learning phase from the keypoint-based representation learning phase. Given the keypoints trajectory $\{z_i^E\}_{i=1}^N$ of the translated robot demonstration video $\{v_i^E\}_{i=1}^N$ and the keypoint-based representation z_t of the current observation O_t , our policy network π outputs an action $a_t = \pi(z_t)$ which is executed in the environment to obtain the next observation O_{t+1} . To achieve physical imitation, we aim to minimize the distance between the keypoints trajectory of the agent and that of the translated robot demonstration video. We define the reward r_t as

$$r_t = d(z_t, z_{t+1}, \{z_i^E\}_{i=1}^N) = \lambda_{r_1} \cdot r_1(t) + \lambda_{r_2} \cdot r_2(t), \quad (8)$$

where λ_{r_1} and λ_{r_2} are hyperparameters that balance the importance between the two terms, and the aforementioned goal is imposed on $r_1(t)$ and $r_2(t)$, which are defined by the following equations:

$$r_1(t) = -\min \|z_t - z_m^E\|, \quad \text{and} \quad (9)$$

$$r_2(t) = -\min \left(\|(z_{t+1} - z_t) - (z_{m+1}^E - z_m^E)\| \right), \quad (10)$$

where $1 \leq m \leq N - 1$, $r_1(t)$ aims to minimize the distance between the keypoint-based representation z_t of the current observation O_t and the most similar (closest) keypoint-based representation z_m^E in the keypoints trajectory $\{z_i^E\}_{i=1}^N$ of the translated robot demonstration video $\{v_i^E\}_{i=1}^N$, and $r_2(t)$ is

the first-order difference equation of $r_1(t)$.

We add the tuple (z_t, a_t, z_{t+1}, r_t) to a replay buffer. Then, the policy network π can be trained with any RL algorithms in principle. We make use of Soft-Actor Critic (SAC) [44] as the RL algorithm for policy learning in our experiments.

V. EXPERIMENTS

In this section, we describe the experimental settings and report results with comparisons to state-of-the-art methods on five robot manipulation tasks. Through experiments, we aim to investigate the following questions:

- 1) How accurate is our perception module in handling the human-robot domain shift and in detecting keypoints?
- 2) How does LbW compare with state-of-the-art baselines in terms of performance on robotic manipulation tasks?

A. Experimental Setting

1. Environment setting. We perform an experimental evaluation in two simulation frameworks, Fetch-Robot manipulation in OpenAI gym [45], and meta-world [46]. We evaluate five tasks: reaching, pushing, sliding, coffee making, and drawer closing.

- 1) For the *reaching* task, the robot has to move its end-effector to reach the target.
- 2) For the *pushing* task, a puck is placed on the table in front of the robot, and the goal of this task is to move the puck to the target location.
- 3) For the *sliding* task, a puck is placed on a long slippery table and the target location is beyond the reach of the robot. The goal of the sliding task is to apply an appropriate force to the puck so that the puck slides and stops at the target location due to the friction.
- 4) For the *coffee making* task, a cup is placed on the table in front of the robot, and the goal of this task is to move

TABLE I: **Success rates** Comparison of success rates for test evaluations of our method LbW and the baselines.

Method	Expert demo	Reaching	Pushing	Sliding	Drawer closing	Coffee making
Classifier reward	35 Robot videos	100%	100%	30%	70%	50%
AVID-m	15 Human videos	100%	60%	0%	50%	40%
LbW (Ours)	1 Human video	100%	100%	80%	80%	70%

the cup to the target, right below the coffee machine outlet. The moving distance of coffee making task is longer than the one in the pushing task.

- 5) For the *drawer closing* task, the robot has to move its end-effector to close the drawer.

At the policy learning phase, the robot receives only an $84 \times 84 \times 3$ RGB image as the observation. The robot is controlled by an Operational Space Controller in the end-effector’s three-dimensional positions. As each of the tasks is described by a single human video, we fix the initial pose of the robot arm and the initial location of the object and the target.

2. Perception Module Training. As we decouple the perception module training and the policy learning phase, we need to collect data for training perception module and the baseline CycleGAN [22]. To generate expert-like behavior in human domain and robot domain for each of the five tasks we follow a specific method to collect data. For human domain, we augment the expert videos with some random behavior. For robot domain, we constraint the action space such that unexpected robot poses will not occur, and then run a random policy to collect data.

The source domain contains human videos with 1056, 398, 650, 986, 658 frames for reaching, pushing, and sliding respectively. The target domain contains robot videos with 3150, 1220, 2120, 2940, 4007 frames for reaching, pushing, sliding, drawer closing, and coffee making respectively. Each frame is a $84 \times 84 \times 3$ RGB image.

B. Comparisons to Baseline Methods

To verify the effectiveness of our perception module fairly, we implement two baselines using the same control model as LbW, which is adopted from [47], but different reward learning methods.

1. Classifier-Reward. We implement a classifier-based reward learning method in a similar way as VICE [48]. For each task, given robot demonstration videos, instead of the human videos, the CNN classifier is pre-trained with goal images with positive labels and the remaining images with negative labels. To learn a policy in the environment, we adopt the implementation from [47], where we use the classifier-based reward to train the agent.

2. AVID-m. To compare our method with AVID [10], we reproduce the reward learning method of AVID and replace the control module with [47], denoted as AVID-m. For each task, given human demonstration videos, we first translate the human demonstration videos to robot domain using CycleGAN [22]. Then the CNN classifier is pre-trained with translated goal images with positive labels and the remaining

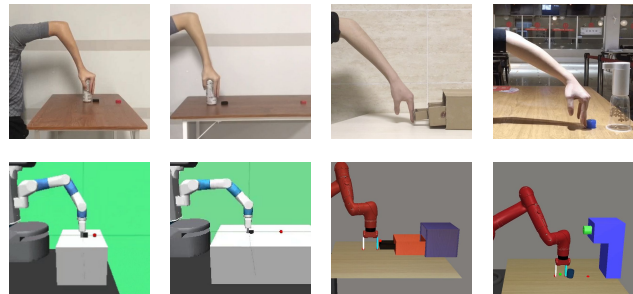


Fig. 5: **Overview of the tasks.** The first row is the example frames of human videos and the second row is the robot observations. Corresponding to each column, from left to right are pushing, sliding, drawer closing, and coffee making tasks.

translated images with negative labels. For the training of RL, we leverage the implementation from [47].

C. Performance Evaluations

Following AVID [10], we use *success rate* as the metric to compare our method with the baselines. At test time, the task is considered to be a success if the robot is able to complete the task within a specified number of time steps (50 time steps for reaching and pushing and 300 time steps for sliding, coffee making, and drawer closing). The results are evaluated by 10 test episodes for each task.

We tabulate the success rate of our method and the two baseline approaches for each of the five tasks in Table I. We find that for the reaching task, all three methods achieve a success rate of 100%. However, as the difficulty of the task increases, the proposed method LbW significantly outperforms the two baseline methods. For the sliding task, the AVID-m method fails to learn the necessary skills for performing the task, while our method outperforms the classifier-based reward learning method. Five quantitative results demonstrate the superiority of our method over competing approaches on all five tasks.

Comparing the classifier-based reward learning method with AVID-m, we discover that AVID-m is very sensitive to the correctness of translated goal images. As shown in Figure 4, there are some visual artifacts in the translated images of AVID-m, heavily influencing the performance of the classifier. As a result, the artifacts would result in predicting meaningless rewards. In contrast, our perception module produces accurately detected keypoints that can endure the artifacts created by translation. The overview of the task scenes and example frames of the human videos can be found in Figure 5. The performance videos of LbW and the comparisons can be found at pair.toronto.edu/lbw-kp/.

VI. CONCLUSIONS AND FUTURE WORK

We introduced LbW, a framework for physical imitation from human videos. Our core technical novelty lies in the design of the perception module that learns human to robot translation followed by keypoint-based representation learning in an unsupervised manner. The resulting representations capture semantically meaningful information that endows the robot the ability to imagine how to perform manipulation tasks in its own context. For controlling the agent with RL, we defined a reward function that encourages the trajectory of the agent to be as close to that of the translated robot demonstration video as possible, with a distance metric in the keypoint space. Experimental results on three robot manipulation tasks demonstrate the effectiveness of our approach and the advantage of learning keypoint-based representations.

However, imitation from a single human video limits the model generalization to novel spatial configurations. For instance, in the pushing task, the initial positions of the puck and target are required to be randomly sampled, instead of being fixed. Moving forward, we aim to learn a policy that is able to push an object from any initial location to any target location from human videos. Thus, learning from a diverse human videos dataset is essential, and is an important future work direction.

REFERENCES

- [1] P. Pastor, L. Righetti, M. Kalakrishnan, and S. Schaal, "Online movement adaptation based on previous sensor experiences," in *IROS*, 2011.
- [2] B. Akgun, M. Cakmak, J. W. Yoo, and A. L. Thomaz, "Trajectories and keyframes for kinesthetic teaching: A human-robot interaction perspective," in *HRI*, 2012.
- [3] T. Zhang, Z. McCarthy, O. Jow, D. Lee, X. Chen, K. Goldberg, and P. Abbeel, "Deep imitation learning for complex manipulation tasks from virtual reality teleoperation," in *ICRA*, 2018.
- [4] S. Calinon, P. Evrard, E. Gribovskaya, A. Billard, and A. Kheddar, "Learning collaborative manipulation tasks by demonstration using a haptic interface," in *ICAR*, 2009.
- [5] A. Mandlekar, Y. Zhu, A. Garg, J. Booher, M. Spero, A. Tung, J. Gao, J. Emmons, A. Gupta, E. Orbay, S. Savarese, and L. Fei-Fei, "Roboturk: A crowdsourcing platform for robotic skill learning through imitation," in *CoRL*, 2018.
- [6] A. Mandlekar, F. Ramos, B. Boots, L. Fei-Fei, A. Garg, and D. Fox, "Iris: Implicit reinforcement without interaction at scale for learning control from offline robot manipulation data," *2020 IEEE International Conference on Robotics and Automation (ICRA)*, pp. 4414–4420, 2020.
- [7] A. Mandlekar, D. Xu, R. Martín-Martín, S. Savarese, and L. Fei-Fei, "Learning to generalize across long-horizon tasks from human demonstrations," *ArXiv*, vol. abs/2003.06085, 2020.
- [8] A. Mandlekar, D. Xu, R. Martín-Martín, Y. Zhu, L. Fei-Fei, and S. Savarese, "Human-in-the-loop imitation learning using remote teleoperation," *ArXiv*, vol. abs/2012.06733, 2020.
- [9] Y. Liu, A. Gupta, P. Abbeel, and S. Levine, "Imitation from observation: Learning to imitate behaviors from raw video via context translation," in *ICRA*, 2018.
- [10] L. Smith, N. Dhawan, M. Zhang, P. Abbeel, and S. Levine, "Avid: Learning multi-stage tasks via pixel-level translation of human videos," in *RSS*, 2020.
- [11] P. Sharma, D. Pathak, and A. Gupta, "Third-person visual imitation learning via decoupled hierarchical controller," in *NeurIPS*, 2019.
- [12] D. Bau, J.-Y. Zhu, J. Wulff, W. Peebles, H. Strobel, B. Zhou, and A. Torralba, "Seeing what a gan cannot generate," in *Proceedings of the IEEE International Conference on Computer Vision*, pp. 4502–4511, 2019.
- [13] B. D. Argall, S. Chernova, M. Veloso, and B. Browning, "A survey of robot learning from demonstration," *Robotics and autonomous systems*, 2009.
- [14] L. Shao, T. Migimatsu, Q. Zhang, K. Yang, and J. Bohg, "Concept2robot: Learning manipulation concepts from instructions and human demonstrations," in *RSS*, 2020.
- [15] P. Sermanet, C. Lynch, Y. Chebotar, J. Hsu, E. Jang, S. Schaal, S. Levine, and G. Brain, "Time-contrastive networks: Self-supervised learning from video," in *ICRA*, 2018.
- [16] D. Pathak, P. Mahmoudieh, G. Luo, P. Agrawal, D. Chen, Y. Shentu, E. Shelhamer, J. Malik, A. A. Efros, and T. Darrell, "Zero-shot visual imitation," in *ICLR*, 2018.
- [17] P. Sermanet, K. Xu, and S. Levine, "Unsupervised perceptual rewards for imitation learning," *arXiv*, 2016.
- [18] T. Yu, C. Finn, A. Xie, S. Dasari, T. Zhang, P. Abbeel, and S. Levine, "One-shot imitation from observing humans via domain-adaptive meta-learning," *arXiv*, 2018.
- [19] X. B. Peng, A. Kanazawa, J. Malik, P. Abbeel, and S. Levine, "Sfv: Reinforcement learning of physical skills from videos," *TOG*, 2018.
- [20] M. Sieb, Z. Xian, A. Huang, O. Kroemer, and K. Fragkiadaki, "Graph-structured visual imitation," in *CoRL*, 2020.
- [21] M. Sieb and K. Fragkiadaki, "Data dreaming for object detection: Learning object-centric state representations for visual imitation," *Humanoids*, 2018.
- [22] J.-Y. Zhu, T. Park, P. Isola, and A. A. Efros, "Unpaired image-to-image translation using cycle-consistent adversarial networks," in *ICCV*, 2017.
- [23] I. Goodfellow, J. Pouget-Abadie, M. Mirza, B. Xu, D. Warde-Farley, S. Ozair, A. Courville, and Y. Bengio, "Generative adversarial nets," in *NeurIPS*, 2014.
- [24] M.-Y. Liu, T. Breuel, and J. Kautz, "Unsupervised image-to-image translation networks," in *NeurIPS*, 2017.
- [25] Y. Choi, M. Choi, M. Kim, J.-W. Ha, S. Kim, and J. Choo, "Stargan: Unified generative adversarial networks for multi-domain image-to-image translation," in *CVPR*, 2018.
- [26] J.-Y. Zhu, R. Zhang, D. Pathak, T. Darrell, A. A. Efros, O. Wang, and E. Shechtman, "Toward multimodal image-to-image translation," in *NeurIPS*, 2017.
- [27] H.-Y. Lee, H.-Y. Tseng, J.-B. Huang, M. Singh, and M.-H. Yang, "Diverse image-to-image translation via disentangled representations," in *ECCV*, 2018.
- [28] X. Huang, M.-Y. Liu, S. Belongie, and J. Kautz, "Multimodal unsupervised image-to-image translation," in *ECCV*, 2018.
- [29] K. Rao, C. Harris, A. Irpan, S. Levine, J. Ibarz, and M. Khansari, "Rl-cyclegan: Reinforcement learning aware simulation-to-real," in *CVPR*, 2020.
- [30] S. James, P. Wohlhart, M. Kalakrishnan, D. Kalashnikov, A. Irpan, J. Ibarz, S. Levine, R. Hadsell, and K. Bousmalis, "Sim-to-real via sim-to-sim: Data-efficient robotic grasping via randomized-to-canonical adaptation networks," in *CVPR*, 2019.
- [31] Y.-C. Chen, Y.-Y. Lin, M.-H. Yang, and J.-B. Huang, "Crdoco: Pixel-level domain transfer with cross-domain consistency," in *CVPR*, 2019.
- [32] S. Gamrian and Y. Goldberg, "Transfer learning for related reinforcement learning tasks via image-to-image translation," in *ICML*, 2019.
- [33] Y. Zhang, Y. Guo, Y. Jin, Y. Luo, Z. He, and H. Lee, "Unsupervised discovery of object landmarks as structural representations," in *CVPR*, 2018.
- [34] T. Jakab, A. Gupta, H. Bilen, and A. Vedaldi, "Unsupervised learning of object landmarks through conditional image generation," in *NeurIPS*, 2018.
- [35] J. Thewlis, H. Bilen, and A. Vedaldi, "Unsupervised learning of object landmarks by factorized spatial embeddings," in *JCCV*, 2017.
- [36] Z. Shu, M. Sahasrabudhe, R. Alp Guler, D. Samarasinghe, N. Paragios, and I. Kokkinos, "Deforming autoencoders: Unsupervised disentangling of shape and appearance," in *ECCV*, 2018.
- [37] O. Wiles, A. Koepke, and A. Zisserman, "Self-supervised learning of a facial attribute embedding from video," *arXiv*, 2018.
- [38] C. Finn, X. Y. Tan, Y. Duan, T. Darrell, S. Levine, and P. Abbeel, "Deep spatial autoencoders for visuomotor learning," in *ICRA*, 2016.
- [39] T. D. Kulkarni, A. Gupta, C. Ionescu, S. Borgeaud, M. Reynolds, A. Zisserman, and V. Mnih, "Unsupervised learning of object keypoints for perception and control," in *NeurIPS*, 2019.
- [40] T. Lesort, N. Díaz-Rodríguez, J.-F. Goudou, and D. Filliat, "State representation learning for control: An overview," *Neural Networks*, 2018.

- [41] A. X. Lee, A. Nagabandi, P. Abbeel, and S. Levine, "Stochastic latent actor-critic: Deep reinforcement learning with a latent variable model," *arXiv*, 2019.
- [42] M. Zhang, S. Vikram, L. Smith, P. Abbeel, M. Johnson, and S. Levine, "Solar: Deep structured representations for model-based reinforcement learning," in *ICML*, 2019.
- [43] D. Hafner, T. Lillicrap, I. Fischer, R. Villegas, D. Ha, H. Lee, and J. Davidson, "Learning latent dynamics for planning from pixels," in *ICML*, 2019.
- [44] T. Haarnoja, A. Zhou, P. Abbeel, and S. Levine, "Soft actor-critic: Off-policy maximum entropy deep reinforcement learning with a stochastic actor," *arXiv*, 2018.
- [45] M. Andrychowicz, F. Wolski, A. Ray, J. Schneider, R. Fong, P. Welinder, B. McGrew, J. Tobin, O. P. Abbeel, and W. Zaremba, "Hindsight experience replay," in *NeurIPS*, 2017.
- [46] T. Yu, D. Quillen, Z. He, R. Julian, K. Hausman, C. Finn, and S. Levine, "Meta-world: A benchmark and evaluation for multi-task and meta reinforcement learning," in *Conference on Robot Learning (CoRL)*, 2019.
- [47] D. Yarats, A. Zhang, I. Kostrikov, B. Amos, J. Pineau, and R. Fergus, "Improving sample efficiency in model-free reinforcement learning from images," *arXiv*, 2019.
- [48] J. Fu, A. Singh, D. Ghosh, L. Yang, and S. Levine, "Variational inverse control with events: A general framework for data-driven reward definition," in *NeurIPS*, 2018.